

Primljen / Received: 28.5.2015.

Ispravljen / Corrected: 9.7.2015.

Prihvaćen / Accepted: 4.8.2015.

Dostupno online / Available online: 10.9.2015.

# Punching strength of flat slabs with and without shear reinforcement

## Authors:



**Marko Bartolac**, PhD CE  
University in Zagreb  
Faculty of Civil Engineering  
[mbartolac@grad.hr](mailto:mbartolac@grad.hr)



Assos.Prof. **Domagoj Damjanović**, PhD CE  
University in Zagreb  
Faculty of Civil Engineering  
[ddomagoj@grad.hr](mailto:ddomagoj@grad.hr)



**Ivan Duvnjak**, PhD CE  
University in Zagreb  
Faculty of Civil Engineering  
[iduvnjak@grad.hr](mailto:iduvnjak@grad.hr)

Subject review

**Marko Bartolac, Domagoj Damjanović, Ivan Duvnjak**

## Punching strength of flat slabs with and without shear reinforcement

The punching shear strength is an extremely significant parameter for the design of flat slabs, i.e. the slabs supported directly on columns, without beams between columns. Slab punching design models are presented according to Eurocode 2, ACI Code 318, and fib Model Code 2010. The authors' own experimental research on the punching shear of slabs with and without shear reinforcement is described, and the results are compared with predictions given in the mentioned design models. It was established that all design models underestimate the experimentally obtained shear strength in the case of slabs without shear reinforcement. As to slabs with shear reinforcement, it was observed that the shear strength determined according to Eurocode 2 is overestimated.

### Key words:

flat slabs, punching, reinforced concrete, shear reinforcement, codes, experiment

Pregledni rad

**Marko Bartolac, Domagoj Damjanović, Ivan Duvnjak**

## Proboj ravnih ploča s posmičnom armaturom i bez takve armature

Nosivost na posmični proboj iznimno je važan parametar pri projektiranju ravnih ploča, odnosno ploča oslonjenih neposredno na stupove, bez greda između stupova. Prikazani su proračunski modeli probvoja ploča prema Eurokodu 2, ACI Codu 318 i fib Model Codu 2010. Opisana su provedena vlastita eksperimentalna istraživanja probvoja ploča s posmičnom armaturom i bez nje te su dobiveni rezultati uspoređeni s predviđanjima spomenutih proračunskih modela. Uočeno je da svi proračunski modeli podcjenjuju eksperimentalno dobivenu nosivost na proboj u slučaju ploča bez posmične armature. Kod ploča s posmičnom armaturom, uočeno je precjenjivanje nosivosti na proboj prema proračunskom modelu Eurokod 2.

### Ključne riječi:

ravne ploče, proboj, armirani beton, posmična armatura, propisi, eksperiment

VÜbersichtsarbeit

**Marko Bartolac, Domagoj Damjanović, Ivan Duvnjak**

## Durchstanzen bei Flachdecken mit und ohne Schubbewehrung

Die Tragfähigkeit gegen Durchstanzen ist ein ausgesprochen wichtiger Parameter im Entwurf von Flachdecken, bzw. bei Platten, die direkt ohne Balkenträger auf den Stützen liegen. Berechnungsmodelle nach Eurocode 2, ACI 318, und fib Model Code 2010 sind dargestellt. Eine Beschreibung durchgeführter experimenteller Untersuchungen zum Durchstanzen bei Platten mit und ohne Schubbewehrung ist gegeben und ein Vergleich zwischen Testresultaten und auf Berechnungsmodellen beruhenden Werten ist aufgestellt. Es wurde festgestellt, dass alle Berechnungsmodelle die experimentell ermittelte Tragfähigkeit gegen Durchstanzen bei Platten ohne Schubbewehrung unterschätzen. Für Platten mit Schubbewehrung scheint das Modell nach Eurocode 2 die Tragfähigkeit zu überschätzen.

### Schlüsselwörter:

Flachdecken, Durchstanzen, Stahlbeton, Schubbewehrung, Regelwerke, Versuche

# 1. Introduction

## 1.1 General data on punching shear

Flat slabs that are supported directly on columns, without beams between the columns, generally transfer a significant concentrated load that affects a relatively small area. The critical element of this system is the slab to column connection because of the concentration of shear stress that is generated in the connection zone, and due to the slab punching risk. The term punching shear denotes slab failure in the zone where the concentrated load is applied, or in the support zone (column) due to shear stress (Figure 1).

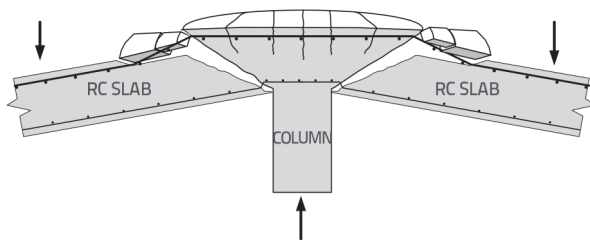


Figure 1. Schematic view of punching in case of slab supported on columns only

At the moment when the punching occurs, the column and slab physically separate from one another, which significantly disturbs the balance of the system formed by these elements. Very often, such disturbance may cause collapse of great proportions due to redistribution of load to other elements that are not designed to transfer such forces (Figure 2). This phenomenon occurs suddenly (brittle fracture), which is why it has to be considered with great care during design of slabs supported on columns only (e.g. in parking garages, office and residential buildings, bridges, etc.), but also in case of slabs lying below columns (e.g., foundation slabs or footings). Although this system requires considerable attention during design, the fact that the slab leans on columns only brings multiple benefits as column capitals or beams are no longer necessary, which results in a simpler and less costly construction (simpler formwork and steel bending plans, easier placement of services/installations, etc.), while also providing an additional free space along the storey height of buildings. Nevertheless, an important deficiency of this structural system must also be mentioned, i.e. the system is prone to considerable deflections. In



Figure 2. Top storey collapse at public carpark in Wolverhampton (UK) [1]

order to avoid brittle failure of slabs by punching shear, slab zones around columns are normally reinforced by means of various reinforcement systems.

According to current regulations, even when calculations prove that the slab need not be reinforced against punching shear, the reinforcement still needs to be placed in the bottom zone of the slab so as to prevent progressive structural collapse resulting from some extraordinary actions (the so called integrity reinforcement). This reinforcement can be in the form of straight or bent bars (Figure 3).

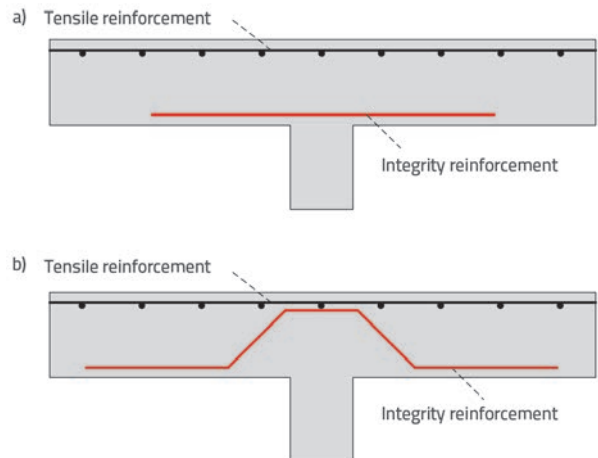


Figure 3. Integrity reinforcement in form of straight and bent bars

The most significant parameters influencing the punching strength of slabs are primarily the compressive strength of concrete, reinforcement ratio, mechanical characteristics and type of reinforcement used, size and geometry of columns, size effect, and effective depth of the slab.

The shear failure of concrete elements without shear reinforcement is directly related to the tensile strength of concrete, which is most often defined as a function of compressive strength. In 1930s author Graf established that no linear relationship exists between the resistance of the slab to column connection and the compressive strength of concrete [2]. According to American regulations ACI Code 318, the punching strength is expressed via the function that is proportional to the square root of compressive strength. However, the expression is used only for concretes whose compressive strength does not exceed 69 MPa, as the punching strength obtained via this expression is overestimated for high strength concretes. In Eurocode 2, the punching strength is expressed via the function that is proportional to the cube root of the compressive strength of concrete.

The reinforcement ratio that is defined as the ratio of the tensile reinforcement area to the effective area of the slab is the parameter that significantly influences punching strength. An increase in the reinforcement ratio also increases the compressive zone, thus reducing the

The reinforcement ratio that is defined as the ratio of the tensile reinforcement area to the effective area of the slab is the parameter that significantly influences punching strength. An increase in the reinforcement ratio also increases the compressive zone, thus reducing the

possibility of crack development due to bending, which enables better transfer of transverse forces in the slab-column connection zone [3]. A greater reinforcement ratio also prevents development of tensile cracks, which is favourable for load transfer via the aggregate interlock mechanism. Authors Kinnunen and Nylander changed the reinforcement ratio on slabs 150 mm in thickness from 0.8 % to 2.1 %, and obtained, by reason of this change, a 95 % increase in punching strength [2].

The stress distribution in the slab to column connection also depends on the dimensions and geometry of columns. The stress concentration occurring in the corners of square and rectangular columns logically causes reduction of punching strength compared to columns of circular cross-section.

## 1.2. Historic development

The first use of reinforced-concrete slabs supported solely on columns dates back to the early twentieth century. This structural system had been developing in America and Europe quite independently from one another. In the US, engineers George M. Hill and C.A. P. Turner are mentioned as being the most deserving for such development [4]. Thus first structures with slabs supported on columns were realized based on the design made by Hill in the period from 1899 to 1901. In the period from 1905 to 1909, Turner used this system on a large number of structures thus proving its safety, and paving the way toward a wider use of this system in the future. A similar structural system was simultaneously developed by Swiss engineer Robert Maillart. In the period from 1900 to 1908, he conducted experimental research on slabs supported on columns. In 1909, he patented his structural system and so a warehouse with RC slabs supported on columns was built in Zurich according to his design [5]. In the same period, Russian engineer Arthur F. Loleit designed a number of structures with slabs supported on columns, and he also ranks among the most deserving engineers that contributed to development of this construction system [6]. Although some difference actually existed in the quantity and distribution of tensile reinforcement, all above mentioned designers used big-size capitals for the transfer of load from slab onto columns, while slabs did not have any special reinforcement to protect them against punching. This construction system is known in literature under the name of "mushroom slabs". This name was

given because of the shape of the column with capital, but also because of the speed of construction which was symbolically compared to the growth of mushrooms.

First attempts to prevent punching by slab reinforcement involved installation of inclined bars bent in the upward direction from the lower zone, which corresponds to the system used for reinforcing beams against transverse forces. Some other reinforcement systems to counter punching were subsequently developed, such as various systems with stirrups, or headed shear stud systems that are now widely used.

During initial application of flat slab systems, the design work was conducted on the empirical level because of insufficient knowledge about failure mechanisms, and about theoretical methods for determination of relevant forces. Westergaard and Slater published in 1921 the first comprehensive theoretical analysis on internal forces for slabs without beams [5]. They determined internal forces within slab using the finite difference method, taking into account various cases of load, and various contributions to the stiffness of columns and capitals. First recommendations for the design of flat slabs, based on experimental research, were given in the US ACI Code for the design of reinforced-concrete structures that was published in 1925.

At that time, the primary aim of researchers was to increase the resistance of slabs against punching. Over time, some other requirements were also formulated by researchers. One of them was the deformation capacity or the capacity to prevent full separation of column and slab after punching. New reinforcement systems for protection against punching were being developed in response to formulation of new requirements.

Kinnunen and Nylander from the Royal Institute for Technology in Stockholm (Sweden) are considered to be the researchers that have set foundations for the modern day computation of punching. The results of their research, published in 1960, considerably affected the knowledge and understanding available at that time with regard to punching action modelling, which subsequently resulted in further development of punching models. Regardless of the fact that their theory was developed for the slabs not specifically reinforced against punching, it served as the basis to numerous researchers who were developing behaviour models for slabs reinforced against punching action. At that time, inclined bars and stirrups were the most frequent forms of such reinforcement.

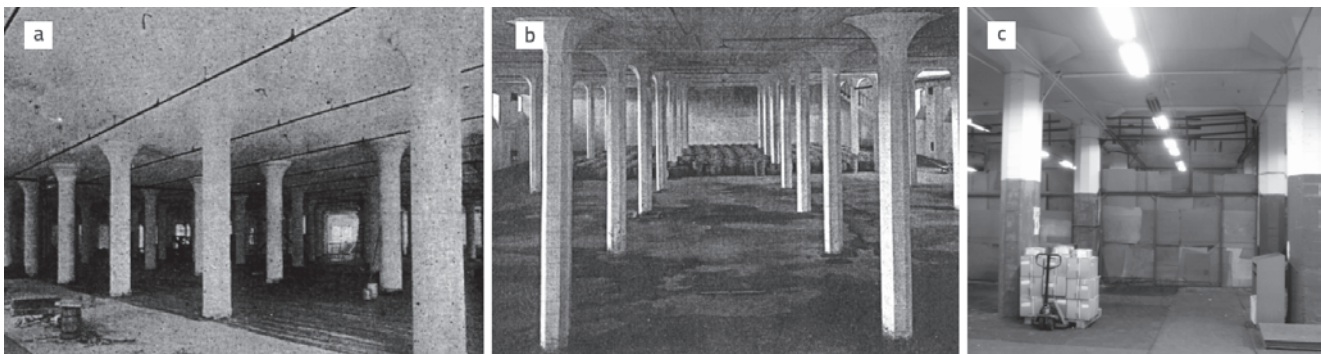


Figure 4. Mushroom slabs: a) C. A. P. Turner, 1909; b) Robert Maillart, 1912; c) A. F. Loleit, 1915 [6]

In the 1970s, many researchers attempted to improve the above-mentioned existing systems for providing reinforcement against punching, as they came to know that proper anchoring of this reinforcement is crucial for preventing the undesired loss of bearing capacity. Among several solutions, the best one was proven to be the solution presented by German researcher Andrä who devised the reinforcement against punching as a set of several vertical bars with anchoring heads aligned along a common metal strip (known as *Dübelleisten* in German). This new system, resembling a sparse comb, initiated an wide array of investigations that have remained unabated to this day. At that, researchers have been attempting to conceive reinforcement systems that can easily and rapidly be assembled on construction site, unlike the slow and complex assembly typical for stirrups. Notable examples are various configurations of prefabricated reinforcement cages or rigid steel elements of varying geometry. In addition, current investigations include various solutions for reinforcing existing structures against punching through installation of various types of reinforcement systems into slabs, which is known as the post installed punching shear reinforcement [7].

Several research groups have been formed worldwide for the study of punching phenomenon for slabs with or without shear reinforcement. The work carried out by some of them will be briefly reviewed in this paper. Thus, the research group from the University of Calgary, Canada, led by professor Dilger who cooperated with the earlier mentioned researcher Andrä, published several papers focusing on this topic [8-11]. The research group from the High Technical School in Aachen, Germany, led by professor Hegger, conducted over the past two decades a number of experimental investigations about the punching of floor slabs and foundations, and it has thoroughly investigated the behaviour of these systems, with and without the punching shear reinforcement, [12, 13]. The

research group that has probably been the most active in recent times is the group from the Federal Polytechnic School from Lausanne, Switzerland, led by professor Muttoni, [14, 15]. The biggest scientific contribution of this group is certainly related to the new theoretical approach to slab punching, which is based on the critical shear crack theory, [16, 17]. According to this theory, the punching shear strength of slabs depends on the slab inclination (rotation) due to load, and the slab stiffness defined through bending strength. The theory is based on the assumption that the punching shear strength reduces with an increase in slab inclination, and it has been incorporated in the Model Code 2010 published by FIB (*Fédération Internationale du béton*).

## 2. Punching shear models

The following regulations for the design of concrete structures were selected to enable comparison with results of the experiments conducted in the scope of this research: Eurocode 2 [18] (hereinafter EC 2), American Concrete Institute's code AC Code 318-14 [19] (hereinafter ACI 318), and fib Model Code 2010 [20] (hereinafter MC 2010). Here it should be noted that the expressions presented in this section may somewhat differ from those given in the above-mentioned codes. This is due to the fact that various safety ratios for actions and material properties have been omitted. In fact, actions are known in the experiment, while properties that have been defined experimentally in advance are used for the materials.

### 2.1. Control (critical) perimeter

The punching shear strength is checked at the control (critical) perimeter. The control perimeter is located at a given distance

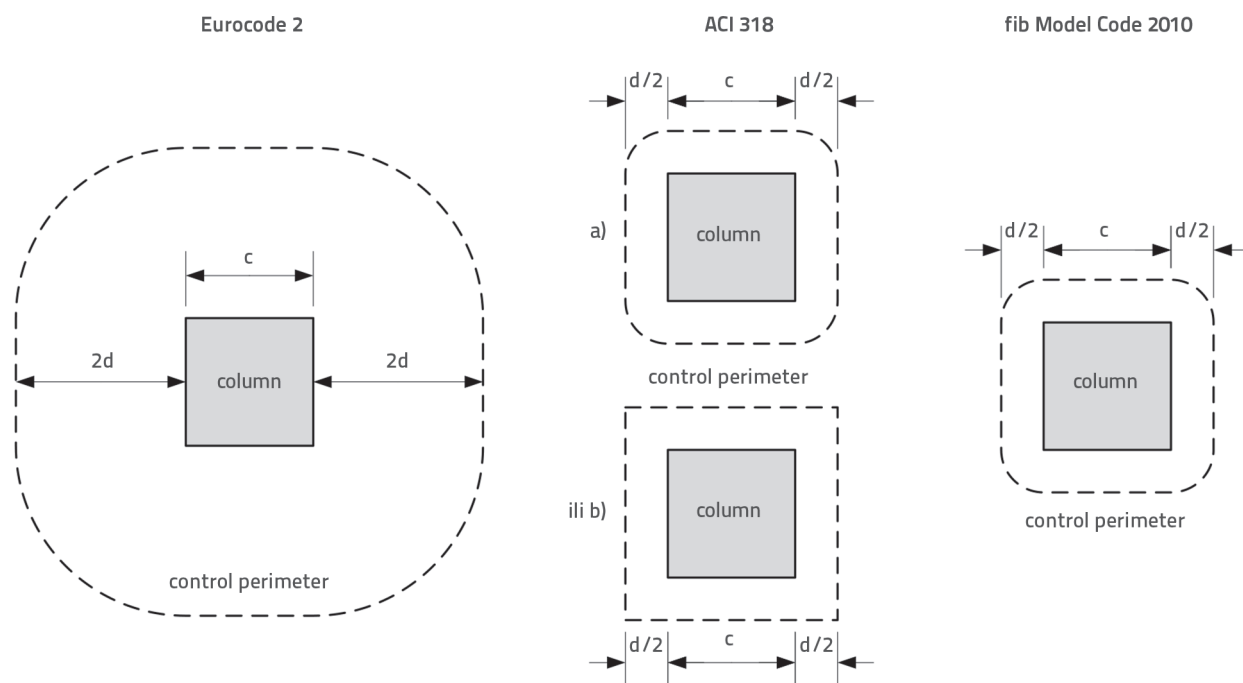


Figure 5. Control perimeter specified in various codes

from the column face. This distance differs in individual codes, varying from one half to double effective depth of the slab. Control perimeters specified in codes used in this paper are presented in Figure 5.

Taking into account provisions presented in Figure 5, control perimeters are calculated according to the following expressions:

- Eurokod 2:  $u = 4 \cdot c + 4 \cdot d \cdot \pi$  (1)
- ACI 318:  $u = 4 \cdot c + d \cdot \pi$  in case a) or  $u = 4 \cdot c + 4 \cdot d$  in case b) (2)
- fib Model Code: 2010  $u = 4 \cdot c + d \cdot \pi$  (3)

where  $c$  is the length of the side of a column of square cross-section, while  $d$  is the effective depth of the slab. As lower control perimeter values result in lower values of the slab punching force, only the value obtained by expression (2) a) will be considered in the rest of the paper for the case of ACI 318 provisions.

## 2.2. Punching forces for slabs without shear reinforcement

According to EC 2, the following expression can be used to calculate punching force for slabs without shear reinforcement:

$$V_{rc} = 0,18 \cdot k \cdot (100 \cdot \rho \cdot f_c)^{1/3} \cdot u \cdot d \quad (4)$$

where  $\rho$  is the ratio of reinforcement for bending,  $f_c$  is the compressive strength of concrete determined on a cylinder, while  $k$  is a dimensionless parameter that takes into account the size effect and is defined by the expression:

$$k = 1 + \sqrt{\frac{200}{d}} \leq 2,0 \quad (5)$$

According to ACI 318, the punching force for slabs without shear reinforcement is calculated according to the expression:

$$V_{rc} = \frac{1}{3} \cdot \sqrt{f_c} \cdot u \cdot d \quad (6)$$

According to MC 2010, the punching force for slabs without shear reinforcement is calculated according to the expression:

$$V_{rc} = k_v \cdot \sqrt{f_c} \cdot u \cdot d \quad (7)$$

The parameter  $k_v$  depends on deformation (or more precisely on slab inclination) and is defined as follows:

$$k_v = \frac{1}{1,5 + 0,9 \cdot k_{dg} \cdot \psi \cdot d} \leq 0,6 \quad (8)$$

Parameter  $\psi$  denotes the slab inclination angle in radians at maximum force, while  $k_{dg}$  takes into account the influence of maximum aggregate grain size in concrete, and is presented according to the following expression:

$$k_{dg} = \frac{32}{16 + d_g} \geq 0,75 \quad (9)$$

where  $d_g$  is the maximum grain size in concrete, i.e. 16 mm in this case.

The slab inclination (rotation) angle  $\Psi$  can be obtained experimentally or by using some theoretical expressions that are proposed according to MC 2010 [20]. The use of a particular theoretical expression depends on the complexity of a given situation for which calculation has to be made and, in this respect, four levels of approximation are differentiated in MC 2010. The following expression for the second level of approximation can be used in the majority of cases [17]:

$$\psi = 1,5 \cdot \frac{r_s \cdot f_y}{d \cdot E_s} \cdot \left( \frac{V_u}{V_{flex}} \right)^{1,5} \quad (10)$$

In expression (10), which is applicable to experimental analysis of punching shear for slabs,  $r_s$  represents radius of a separated slab element in mm (distance between the column axis and slab edge – 750 mm in this paper),  $f_y$  is the yield strength for bending reinforcement,  $E_s$  is the elastic modulus of reinforcing steel,  $V_{flex}$  is the maximum force during testing, a  $V_{flex}$  is the force causing failure of bending reinforcement in the zone below (or above) the column. The force  $V_{flex}$  can be calculated using the following expression:

$$V_{flex} = \frac{4 \cdot m_R}{r_q \cdot \left( \cos \frac{\pi}{8} + \sin \frac{\pi}{8} \right) - c} \cdot \frac{B^2 - B \cdot c - c^2 / 4}{B - c} \quad (11)$$

where  $r_q$  is the radius in which reaction forces occur on slab, in mm (750 mm in this paper),  $c$  is the length of the square column side in mm,  $B$  is the length of the slab side in mm, and  $m_R$  is the maximum bending moment of the slab per meter of width in Nmm (nominal capacity of the slab bending moment). Assuming an ideal plastic behaviour of reinforcement after yielding, and a rectangular form of concrete stress diagram in compression zone, while neglecting the reinforcement in the compression zone, the value of the moment  $m_R$  can be obtained using the following expression:

$$m_R = \rho \cdot f_y \cdot d^2 \cdot \left( 1 - \frac{\rho \cdot f_y}{2 \cdot f_c} \right) \quad (12)$$

## 2.3. Punching forces for slabs with shear reinforcement

All codes presented in this paper assume joint action of concrete and shear reinforcement in slabs subjected to punching shear. This can generally be presented as follows:

$$V_{rd} = V_{rc} + V_{rs} \quad (13)$$

However, the components given in the preceding expression (13) differ in individual codes, and the difference is especially striking between the concept adopted in EC2 and ACI 318 on the one side, and that used in MC 2010, on the other. According to EC 2, the punching force for slabs with shear reinforcement can be calculated as follows:

$$V_{rd} = 0,75 \cdot 0,18 \cdot k \cdot (100 \cdot \rho \cdot f_c)^{1/3} \cdot u \cdot d + 1,5 \cdot \frac{A_{sw} \cdot f_{ywd,ef} \cdot d}{s_r} \quad (14)$$

where  $A_{sw}$  is the total area of shear reinforcement along one column perimeter in mm<sup>2</sup>,  $s_r$  is the radial distance between

individual shear reinforcement perimeters in mm, and  $f_{ywd,ef}$  is the allowable design stress of shear reinforcement as given in the following expression:

$$f_{ywd,ef} = 250 + 0,25 \cdot d \leq f_{ywd} \quad (15)$$

According to ACI 318, the punching force for slabs with shear reinforcement is calculated according to the following expression:

$$V_{rd} = \frac{1}{6} \cdot \sqrt{f_c} \cdot u \cdot d + \frac{A_{sw} \cdot f_{yt} \cdot d}{s_r} \quad (16)$$

where the parameters  $A_{sw}$  and  $s_r$  have the same meaning as in Eurocode 2, while the allowable design stress of shear reinforcement  $f_{yt}$  is limited to 414 MPa (60 000 psi). Certain similarities can be observed by comparing expressions (4) and (14), and (6) and (16). In the first place, both codes reduce bearing capacity of concrete as related to slabs that are not reinforced with shear reinforcement. Thus this value is reduced for 25 % in EC 2, i.e. for 50 % in ACI 318. The 25 % reduction is allowed according to ACI 318 but only if shear reinforcement with anchoring heads, i.e. headed shear studs, are used. This reduction is due to the assumed wider shear cracks in slabs reinforced with shear reinforcement compared to the slabs that are not reinforced with shear reinforcement [14]. Wider cracks lead to a reduced capacity of concrete to transfer shear, which is primarily due to a reduced possibility of an efficient interlocking of aggregate grains that are situated on two opposite sides of the shear crack. Secondly, the right-side addends in expressions (14) and (16) have a very similar form, and they differ in the size of allowable design stress of shear reinforcement, and in the ratio by which the addend is multiplied (1.5 in Eurocode 2, and 1.0 in ACI 318). This ratio takes into account the shear-reinforcement efficiency. According to MC 2010, the contribution of shear reinforcement to the bearing capacity of slab subjected to punching shear can be calculated using the expression:

$$V_{Rs} = \sum A_{sw} \cdot k_e \cdot \sigma_{sw} \quad (17)$$

where  $\sum A_{sw}$  is the total area of shear reinforcement that is intersected by the potential shear crack (under an angle of 45°) within an area between 0,35 · d and d (d is the effective depth of the slab),  $k_e$  is the ratio that takes into account the column position, i.e. the influence of possible force eccentricity (0.9, 0.7, and 0.65, for the central, peripheral and corner columns, respectively), and  $\sigma_{sw}$  is the stress in shear reinforcement that is calculated according to the expression:

$$\sigma_{sw} = \frac{E_s \cdot \psi}{6} \cdot \left( 1 + \frac{f_{bd}}{f_{yw}} \cdot \frac{d}{\phi_w} \right) \leq f_{yw} \quad (18)$$

In the expression (18),  $\phi_w$  is the shear reinforcement diameter, while  $f_{yw}$  is the yield strength of shear reinforcement. The parameter  $f_{bd}$  is the bond strength of reinforcement that can be

taken to be 3 MPa for practical uses. MC 2010 also contains expressions for an accurate calculation of this parameter in concrete cases. At this point, it should be noted that MC 2010 does not anticipate reduction of shear strength of concrete in case of slabs with shear reinforcement, as related to those without shear reinforcement, in the manner such reduction is defined in EC 2 and ACI 318. Instead of reduction defined by a constant value, MC 2010 anticipates reduction in the concrete contribution by an increase in the slab inclination angle.

### 3. Experimental research

#### 3.1 Mechanical properties of materials

The concrete composition presented in Table 1 was used in the scope of experimental research. The following river aggregate fractions were used in the preparation of concrete: 0 – 4 mm (crushed river aggregate), 4 – 8 mm, and 8 – 16 mm. The cement type CEM II/A-M 42,5 N was used. The superplasticiser type BASF MasterGlenium 51 was used to achieve better workability, i.e. the target consistency class S4. The measured slump of fresh concrete ranged from 160 to 190 mm.

Properties of reinforcement used in the research were determined experimentally, by tensile testing according to HRN EN 15630-1 [21]. Deformed reinforcement of 14 mm in diameter and with yield strength of  $R_{p0,2} = 560$  MPa was used. For punching shear reinforcement, deformed bars 6 mm in diameter, with the yield strength of  $R_{p0,2} = 508$  MPa were used. The elastic modulus  $E_s$  of the reinforcing steel amounted to 200 GPa.

Table 1. Composition of concrete mix

Cement [kg/m³]	Water [l/m³]	Aggregate, total [kg/m³]	v/c ratio	Superplasticizer [kg/m³]
370	170	1840	0.46	2.22

Basic mechanical properties were determined experimentally. The compressive strength of concrete ( $f_{ck}$ ) was tested on 150 mm cubes in accordance with HRN EN 12390-3 [22]. The elastic modulus of concrete was determined on cylinders 150 mm in diameter and 300 mm in height, according to HRN EN 12390-13 [23]. The stabilised secant elastic modulus ( $E_{cs}$ ) was determined based on the method B given in the mentioned standard, through measurement of strain on three points along the cylinder area (these three points together close an angle of 120°). After the elastic modulus testing, the same cylinders were used to determine the tensile strength of concrete using the splitting method ( $f_{ctm,sp}$ ) according to provisions contained in HRN EN 12390-6 [24]. The tensile strength of concrete ( $f_{ctm,fl}$ ) was also determined experimentally by bending prismatic specimens measuring 150 x 150 x 600 mm in three points with an initial 25 mm notch at half span. Force – displacement diagrams for concrete specimens from every slab, and testing photographs, are presented in Figure 6.

Compressive strength values for concrete, determined as average values from results obtained by testing three cubes

Table 2. Test results for elastic modulus, compressive and tensile splitting strength of concrete

Slab	Compressive strength [MPa]			Tensile splitting strength [MPa]	Elastic modulus [GPa]	Tensile bending strength [MPa]
	$f_{ck}$	$\sigma$	V (%)	$f_{ctm,sp}$	$E_{c,s}^b$	$f_{ctm,fl}^b$
S1-1	49.7	1.1	2.21	3.5	33.4	3.93
S1-2	53.3	1.6	2.93	3.4	37.0	4.30
S1-3	51.0	1.4	2.72	3.0	36.6	3.96
Average for slab S1	51.3	1.4	2.62	3.3	35.7	4.1
S2-1	54.1	1.3	2.36	3.1	36.5	4.30
S2-2	50.4	0.4	0.72	3.5	35.5	3.95
S2-3	52.8	1.0	1.81	3.2	34.7	4.36
Average for slab S2	52.4	0.9	1.63	3.3	35.6	4.2

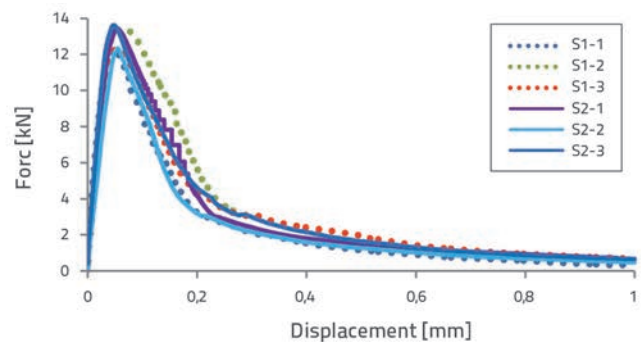


Figure 6. Tensile bending strength: a) concrete prism testing; b) force – displacement diagram

for every slab, and the corresponding standard deviation ( $\sigma$ ) and variation ratio (V) values, are presented in Table 2. The tensile splitting strength, elastic modulus, and tensile bending strength values, defined by testing one specimen for each slab, are presented in the same table. The results are divided into two groups: S1 – concrete for slabs with shear reinforcement, and S2 – concrete for slabs without shear reinforcement.

### 3.2. Slab specimens for testing

A total of six slabs were tested in the scope of this research. Three of them (marked S1) were reinforced against punching shear, and no reinforcement against punching shear was provided for the remaining three slabs (marked S2). Although state of the art research shows that usually one specimen is tested, the authors of this paper consider that this is insufficient for accurate interpretation of subsequent analyses of results obtained through various design models. That is why it is advisable to test at least two similar specimens during the conduct of this type of experiments.

All slabs subjected to this testing had similar dimensions, and were made of concrete of similar composition. Slab dimensions of 1.50 x 1.50 x 0.125 m represent models on the scale of 1/2 with respect to the real slab system supported solely on columns has a zero point at approximately 0,22·L

from the column axis (L denotes the slab span length), then the tested specimens represent the slab system 25 cm in thickness, supported on columns spaced at approximately 7 m, for which the span/thickness ratio is about 28. Plan dimensions of the steel slab over which the concentrated load was applied amounted to 13 x 13, i.e. it represented a real column of a square cross section measuring 26 x 26 cm.

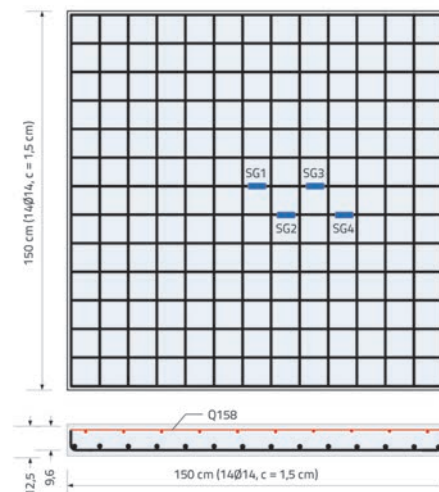


Figure 7. Principal reinforcement in slab and disposition of strain gauges

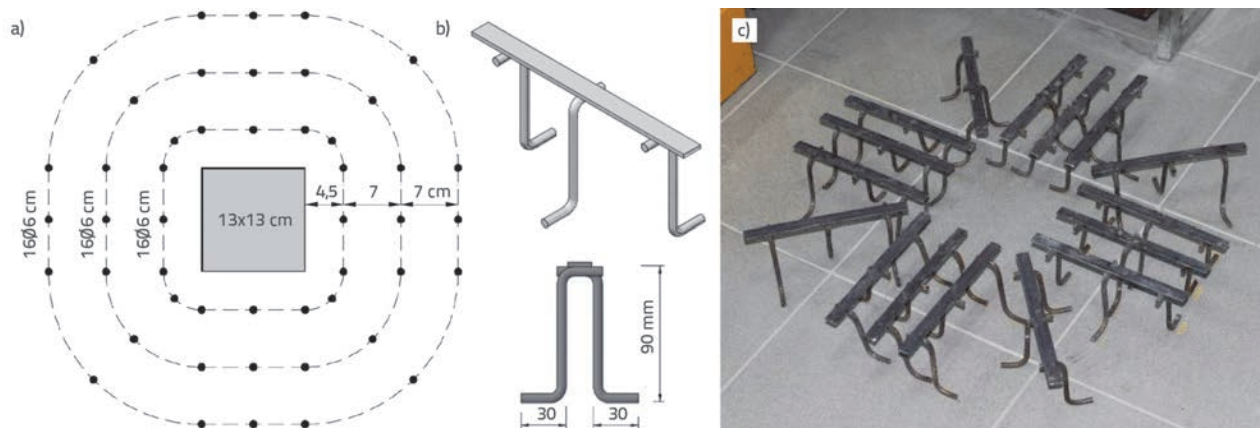


Figure 8. Punching reinforcement for slab type S1: a) distribution of reinforcement; b) dimensions; c) photo showing arrangement prior to installation

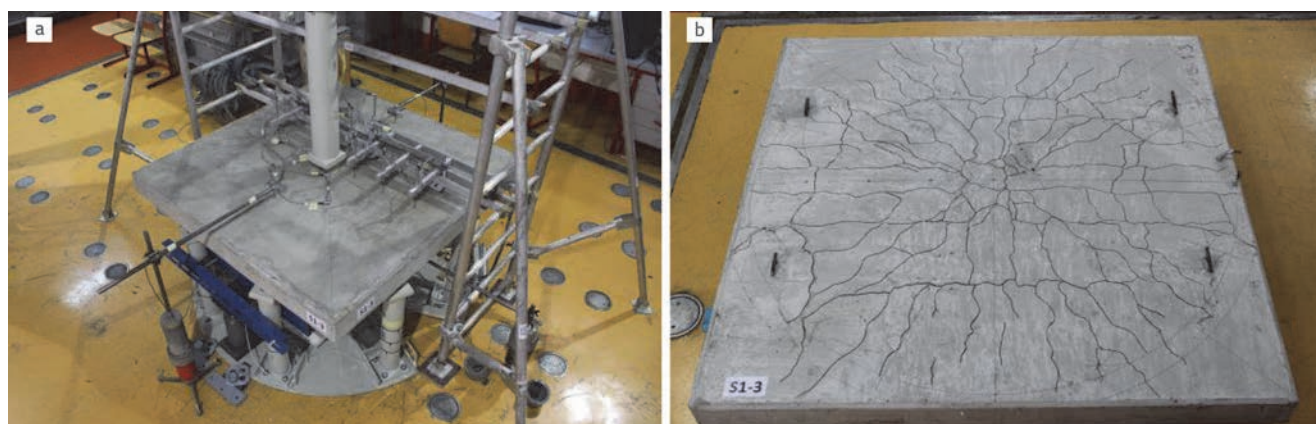


Figure 9. Slab S1-3: a) during the testing; b) tensile side after testing

In order to prevent bending failure of slab specimens, and to enable failure due to punching effect, it was necessary to add more reinforcement to the slab compared to the quantity normally used in practice. The reinforcement ratio was 1.5 %, and the reinforcement 14 mm in diameter, spaced at 11 cm, was selected. The steel mesh fabric Q158, consisting of 5.5 mm bars spaced at 15 cm in both directions, was placed at the compression side. The protective layer of concrete was 1.5 cm on the tension side and 2.0 cm on the compression side, while the intermediate effective depth of the slab amounted to 9.6 cm. The arrangement of slab reinforcement in plan and cross-section is shown in Figure 7. To control stress in reinforcement system during the testing, four strain gauges were placed on tensile reinforcement in one slab for each slab type, before the concreting. The stress values in reinforcement at the moment of failure are the real indicator of whether the slab failed due to bending or punching.

As already indicated, type S1 slabs contained the punching reinforcement in addition to the bending reinforcement. It was established by previous calculation according to Eurocode 2 guidelines that the punching reinforcement has to be provided in three perimeters, as shown in Figure 8.a.

The system made of three vertical reinforcing bars 6 mm in diameter, with hooks 3 cm in length at an angle of 90°, was

used for reinforcement against punching shear. These three bars were then welded via hooks onto a metal strip measuring 16 x 3 mm at 7 cm intervals (Figures 8.b and 8.c). This reinforcement system was used to try to simulate currently the best form of reinforcement against punching – vertical bars with anchoring heads (headed shear studs) mentioned in the first section, which are not produced for such low slab thicknesses.

### 3.3. Test setup and measurements

A steel frame consisting of eight steel columns of circular cross section was fabricated for the slab testing. The slabs were discretely positioned into this frame via spatially hinged supports (Figure 9). Columns (supports) were placed in the radius of 75 cm from the centre of the slab. The load was applied continuously until failure with controlled displacement ( $v = 0.4$  mm/min) using a hydraulic static-dynamic testing machine, 600 kN in capacity. A HDF plate (high-density fibreboard of approximately 850 kg/m<sup>3</sup>) of equal dimensions (13 x 13 cm) was placed below the load transferring steel plate, in order to prevent stress concentration at the edges of the plate. Prior to each testing, a considerable attention was paid to proper placing of specimens into the frame, i.e. to symmetric positioning of specimens onto all supports.

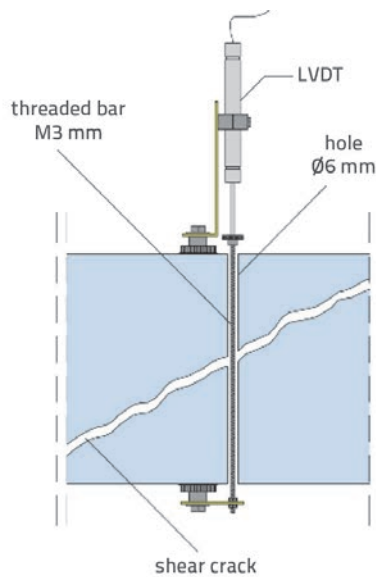


Figure 10. Placement of sensors for measuring change in slab thickness

The force and various other slab behaviour parameters were continuously measured during the testing. Measurement points on slabs are shown in Figures 11.a and 11.b.

A total of 12 linear variable differential transformers (LVDTs) for measurement of vertical displacements were placed on the top and bottom surfaces of the slabs. On the top side of the slab, displacements were measured along two axes (A and B), and this on three points along each axes – in one-eighths and one-fourths of the span (measurement points G1A to G3A and G1B to G3B). To control the slab displacement symmetry, displacements were also measured in one-fourths

of span in axes C and D (measurement points G2C and G2D). On the bottom side, displacements were measured along the axis A only, and this at four points – in one-eighths, in one-fourth and one-half of the slab span (measurement points DOA to D3A).

In addition, two LVDTs were used to measure the slab thickness during the testing (measurement points PC and PBC). Two holes 6 mm in diameter were left in all slabs during concreting to enable installation of these LVDTs. Thin threaded bars (3 mm in diameter) were then passed through these holes and fixed on the bottom side of specimens. On the top side of specimens, the threaded bars were connected with the LVDT fixed on the top side of the slab (Figure 10).

Radial strain were measured solely on the compression side of slabs by inductive sensors placed on the measurement base of 100 mm. Sensors were placed in two directions, along the axes C and AD (diagonally between the axes A and D), as shown in Figure 11.a. The occurrence of decompression (reduction of compression deformation) on these measurement points is an indicator of development of shear cracks, i.e. of the oncoming punching shear failure.

### 3.4. Test results

A total of three type S1 slabs marked S1-1, S1-2 and S1-3 (with shear reinforcement), and three slabs marked S2-1, S2-2 and S2-3 (without shear reinforcement), were tested. Some selected measurement results for displacement and strain, and rotation angles calculated from measured displacements, are given below.

Measured punching shear results (maximum force during testing), and some of the measured displacements and rotation

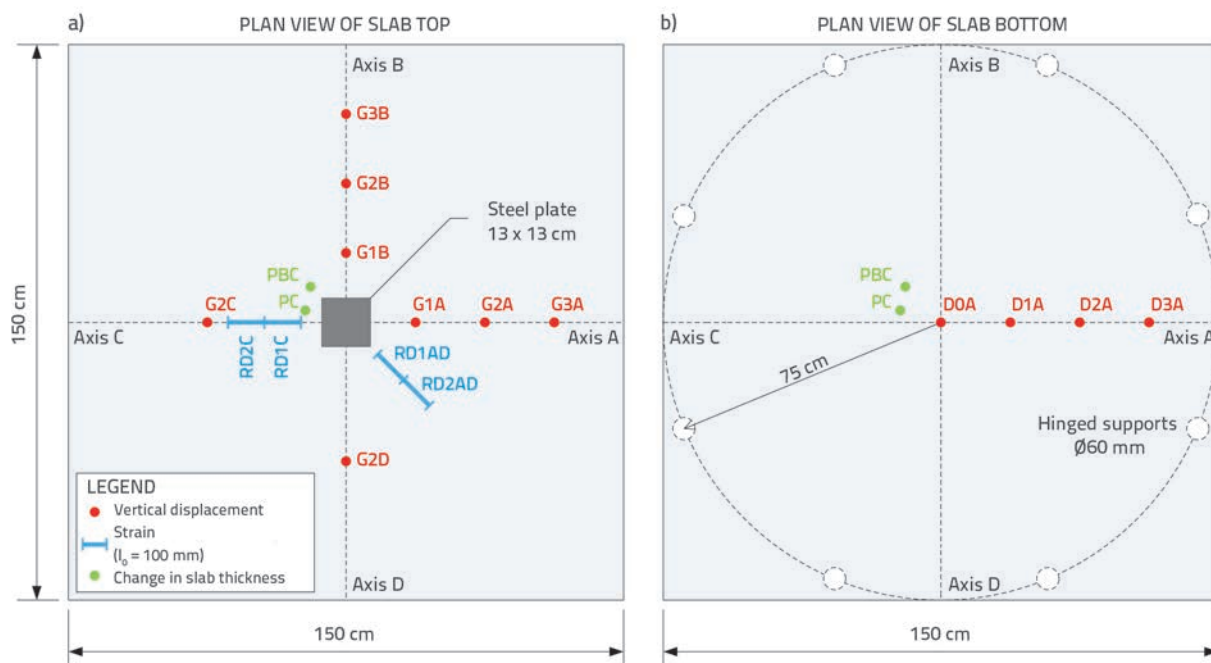


Figure 11. Plan view of measurement points on slabs: a) top side; b) bottom side

Table 3. Maximum forces and some displacements and inclination angles immediately prior to punching shear

Slab	$F_{max}$ [kN]	Displacement DOA [mm]	Displacement G1A [mm]	Displacement G1B [mm]	$\Psi_{max, exp}$ [rad]
S1-1	393.9	18.7	14.9	14.0	-0.0227
S1-2	361.3	17.1	13.8	12.8	-0.0213
S1-3	385.2	17.2	14.2	13.4	-0.0205
Average for slab S1	380.2	17.6	14.3	13.4	-0.0215
$\sigma$	16.9	0.9	0.5	0.6	0.0011
S2-1	345.2	14.2	11.7	11.4	-0.0178
S2-2	303.3	11.5	9.4	8.9	-0.014
S2-3	328.4	13.4	10.7	10.4	-0.0157
Average for slab S2	325.6	13.0	10.6	10.2	-0.0158
$\sigma$	21.1	1.4	1.1	1.2	0.0019

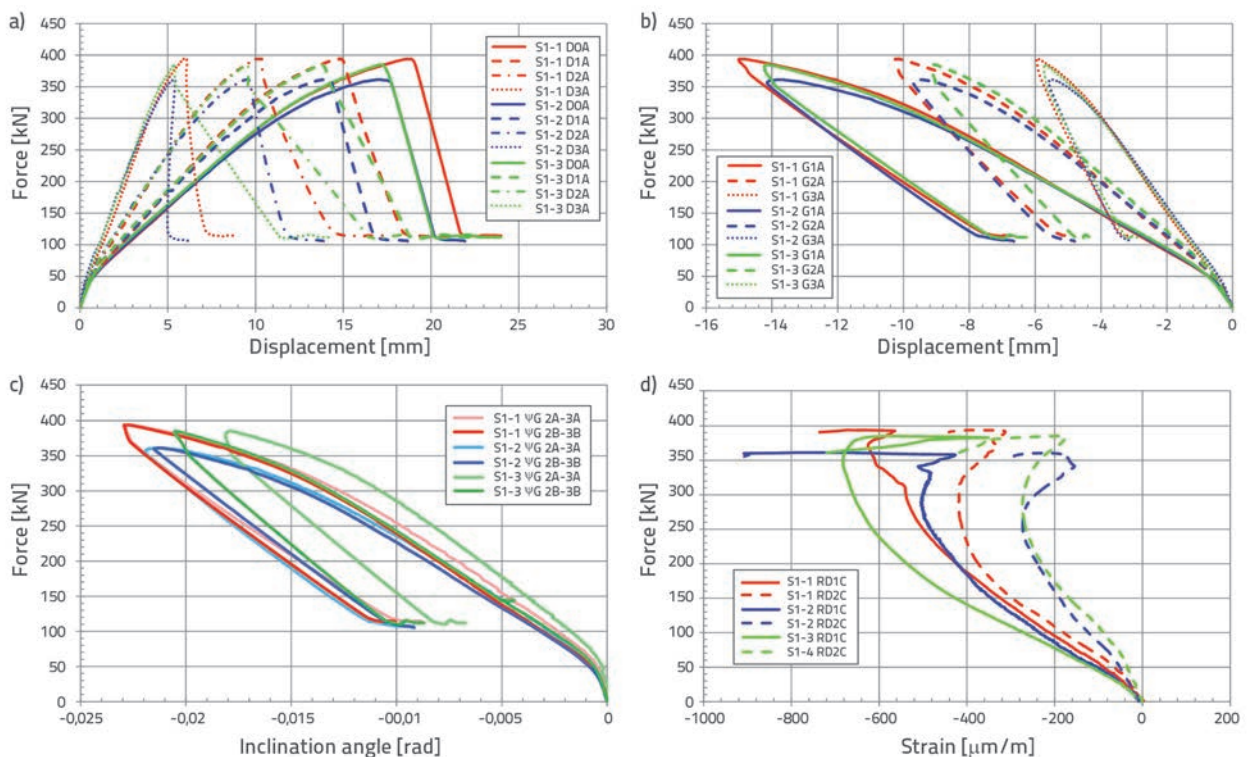


Figure 12. Slabs S1: a) force – displacement (line A below); b) force – displacement (line A above); c) force – inclination angle (lines A and B above); d) force – strain (line C above)

angles determined at that moment (immediately prior to punching), are presented in Table 3.

Although several slab rotation angles can be expressed based on measurement results, it was decided that the rotation angles of interest are those between the points G2A and G3A, and G2B and G3B. The greater angle, shown in Table 3, was selected as relevant angle. Rotation angle represents the deformation capacity of the slab.

Test results for slab S1 and S2 are shown in Figures 12 and 13, respectively.

In general terms, the behaviour of specimens taken from both slab types can be considered as quite uniform, with some greater deviations in case of the slab without shear reinforcement, as might have been expected. It can be seen from the diagrams that the failure occurred by brittle fracture – punching failure. In addition, two areas can be differentiated in the diagrams: linear area with an initial stiffness corresponding to pre-cracking conditions, and area in which the slab stiffness was reduced due to occurrence of cracks. Force – displacement diagrams (Figures 12.a and 12.b, 13.a and 13.b) show a clear

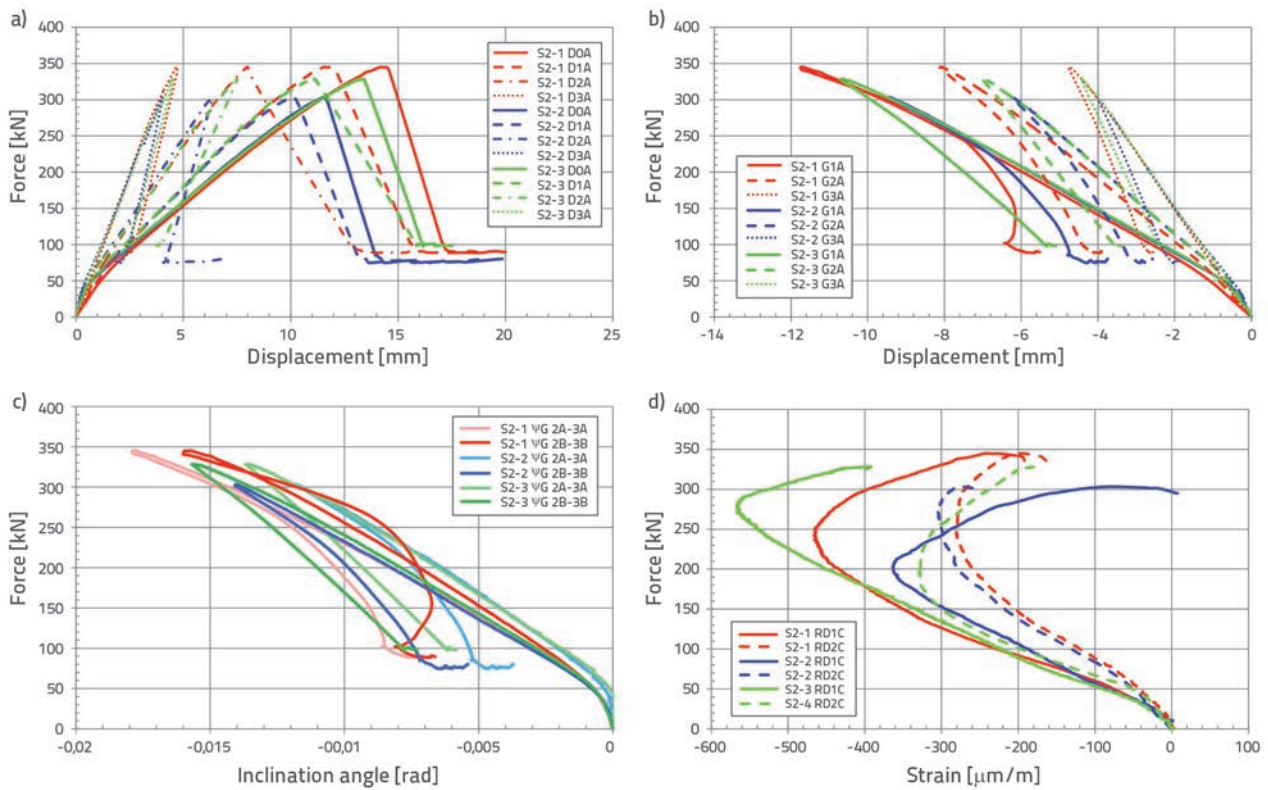


Figure 13. Slabs S2: a) force - displacement (line A below); b) force – displacement (line A above); c) force – inclination angle (lines A and B above); d) force – strain (line C above)

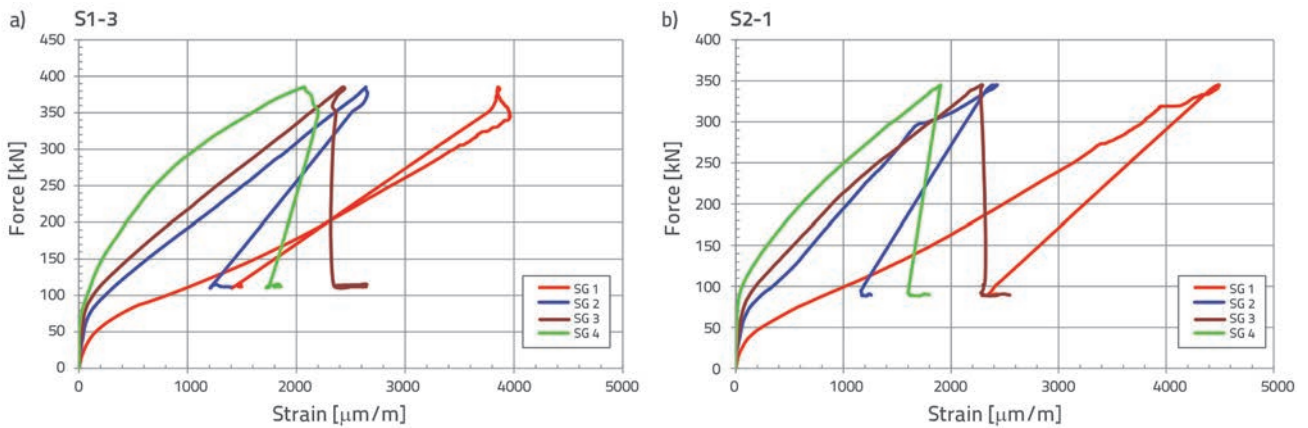


Figure 14. Strain on tensile reinforcement: a) slab S1-3; b) slab S2-1

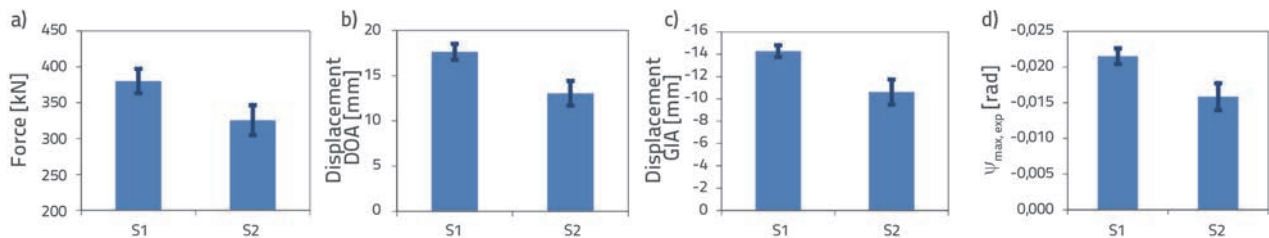


Figure 15. Average values: a) punching forces; b) displacements on line A below; c) displacements on line A above; d) maximum inclination angle

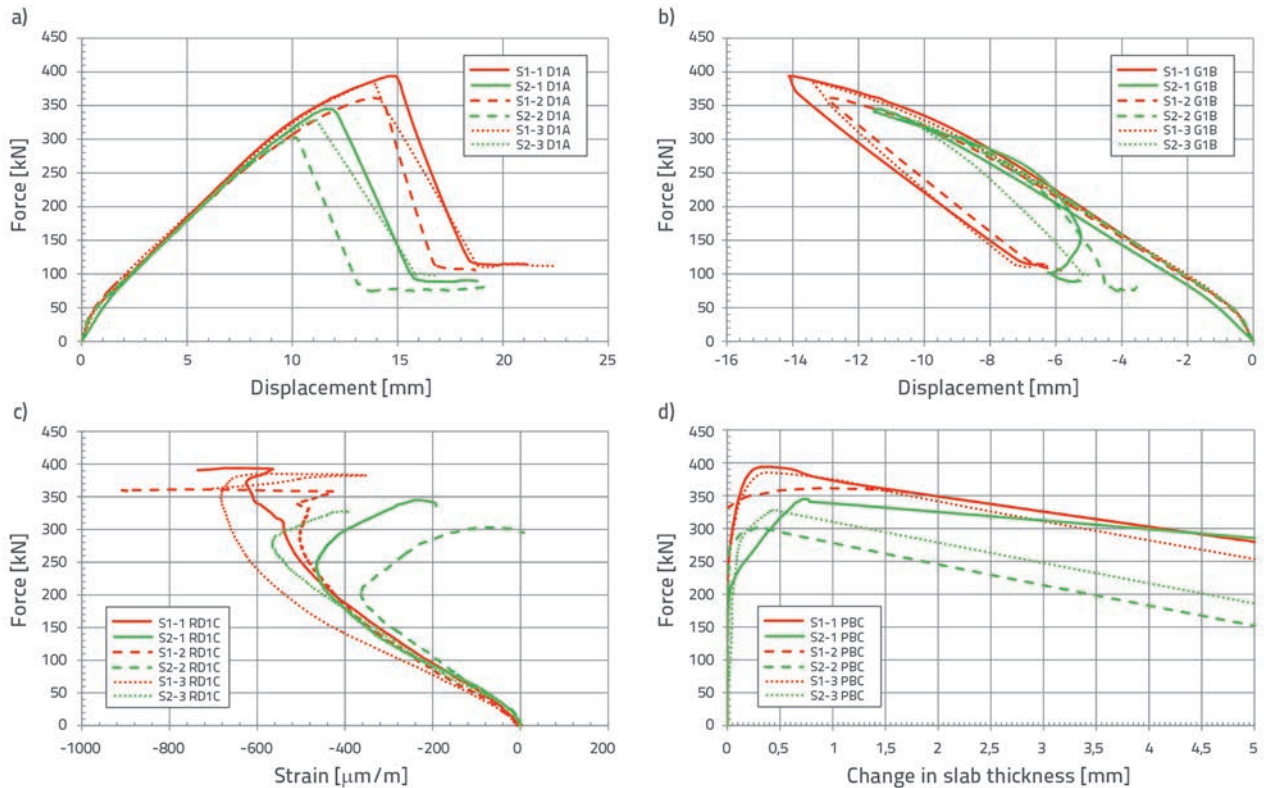


Figure 16. Slabs S1 and S2: a) force - displacement D1A; b) force – displacement G1B; c) force – strain at RD1C; d) force – change of thickness at PBC slab

distribution of displacements along individual axes. Force – inclination angle diagrams (Figures 12.c and 13.c) show differences between the selected inclination angles. Force – relative deformation diagrams (Figures 12.d and 13.d) reveal reduction of compression deformations due to formation of a punching cone (pyramid), i.e. due to indications of imminent punching failure.

Measurements of strain of reinforcement on slabs S1-3 and S2-1, which show that the yielding of tensile reinforcement did not occur during the testing, are shown in Figure 14.

Figure 15 shows average punching force values and D0A and G1A displacements (bottom and top sides of slabs) and maximum

inclination angles immediately prior to punching failure. From this it can be concluded that the punching shear strength and deformation capacity of slabs with shear reinforcement is higher as related to slabs without shear reinforcement. An average increase in the punching strength and the deformation capacity (inclination angle) amounts to 17 % and 36 %, respectively.

Diagrams presented in Figure 16 show displacement measurements for measurement points D1A and G1B, strain measurements for the measurement point RD1C, and slab thickness change at the measurement point PBC, as related to force for all tested slabs. It can be seen from the force – displacement diagrams given in Figure 16 that the slab bending

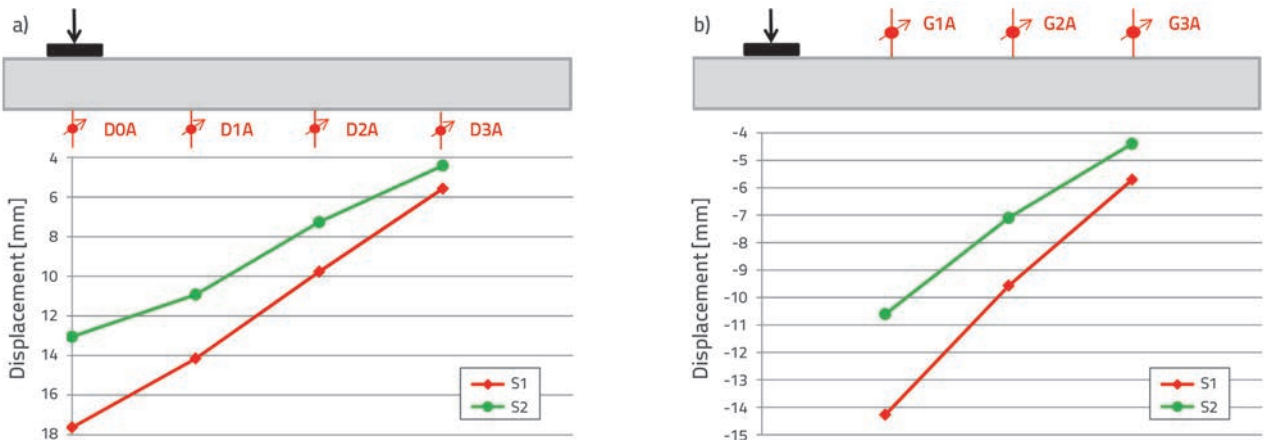


Figure 17. Average displacements along line A (below and above) for both slab types immediately prior to punching failure

stiffness does not change by installation of shear reinforcement, and that slabs with shear reinforcement exhibit greater load bearing capacity values after failure.

It can be noticed on the force – strain diagram given in Figure 16.c that the decompression in compression zone (i.e. creation of punching cone) starts considerably before the actual failure in case of slabs without shear reinforcement. The situation is somewhat different for slabs with shear reinforcement as the reinforcement prevents (limits) creation of punching cone in the form in which it occurs in case of slabs without shear reinforcement.

The measurement of change in slab thickness can also be interpreted as an indirect measurement of the shear crack width. The difference in this parameter between slabs with and without shear reinforcement can be seen in the force – slab thickness change diagram in Figure 16.d. In fact, in case of specimens without shear reinforcement, the sudden change in slab thickness occurs immediately after occurrence of the first shear crack. On the other hand, in case of slabs with shear reinforcement, this enables a controlled spreading of shear cracks in the area prior to and immediately after the punching force is attained..

A graphical presentation of average displacement along the line A (below and above) is shown in Figure 17 for both slab types, immediately prior to punching failure.

After the end of testing, one slab was taken from each slab type and cut in two pieces so that the difference in the form of punching cone can be observed (Figure 18). It can be seen that the shear reinforcement in the slab S1-1 caused reduction of the shear crack angle as related to the slab S2-2 (from  $\approx 45^\circ$  to  $\approx 15^\circ$ ), i.e. that it activated a much greater slab area for resistance to concentrated action in the centre of the slab.



Figure 18. Slabs S1-1 and S2-2 cut after testing

## 4. Comparison of test results and calculation models

### 4.1. Input data for calculation

Some of the basic parameters and assumptions used in calculation of both slab types, which have not been discussed in previous parts of the paper, are presented in this section.

To enable comparison between the slab testing results and calculation model results, the value of 1 was assumed in calculation models for all safety ratios relating to material properties and actions. This is a standard procedure in cases when all input parameters are known, i.e. when they have been experimentally determined by one's own testing.

As explained in section 3, the compressive strength of concrete is determined for each slab based on compressive strength testing conducted on three cubes 28 days after concreting. As slabs were not tested on the day the mentioned cubes were tested, the increase in compressive strength of concrete until the slab testing date was estimated according to the corresponding expression given in EC 2 [18]. Calculated compressive strength values used in design models are shown in Table 4. It should be noted that these values are related to the compressive strength used in all design models, which amounts to eighty percent of the compressive strength determined on cubes.

Table 4. Slab age on testing day and compressive strength estimate

Slab	Slab testing date	Slab age on testing date* [dani]	Estimated compressive strength on testing day [MPa]
S1-1	27.4.2015.	60	43.1
S1-2	15.4.2015.	48	45.2
S1-3	9.4.2015.	42	42.7
S2-1	8.4.2015.	41	45.2
S2-2	30.4.2015.	63	43.8
S2-3	13.4.2015.	46	44.6

\* Slabs were cast on 26 February 2015

The concept of critical (control) perimeter is explained in Section 2, where expressions for calculation of this parameter according to individual codes are also given. Assuming the mean effective depth of 96 mm and the column side length of 130 mm, the following control perimeter values are obtained:

- Eurokod 2, expression (1): 1726 mm
- ACI 318, expression (2) a): 822 mm
- fib Model Code 2010, expression (3): 822 mm

At this point, we should also consider the contribution of slab self-weight to the experimentally determined punching forces. The part of the slab that participates in shear transfer can be regarded as a truncated cone or pyramid whose volume can be calculated. In fact, the truncated cone is usually mentioned in literature although the base in the zone of force application (compression side) is actually of square form, while it is of irregular approximately circular form on the tensile side. It is usually assumed that the surface area of the cone (pyramid) is situated at an angle of  $\approx 30^\circ$  with respect to the slab plane and so, once the calculated volume is multiplied with the

**Table 5. Comparison of experimental results and values calculated according to various codes (slabs without shear reinforcement)**

Slab	$f_c$ [MPa]	$\Psi_{\text{exp, max}}$ [rad]	$V_{\text{exp}}$ [kN]	$V_{\text{EC2}}$ [kN]	$V_{\text{ACI}}$ [kN]	$V_{\text{MC}}$ [kN]	$V_{\text{exp}}/V_{\text{EC2}}$	$V_{\text{exp}}/V_{\text{ACI}}$	$V_{\text{exp}}/V_{\text{MC}}$
S2-1	45.2	0.0178	345.2	243.3	176.8	174.6	1.42	1.95	1.98
S2-2	43.8	0.0140	303.3	240.8	174.0	192.5	1.26	1.74	1.58
S2-3	44.6	0.0157	328.4	242.2	175.6	184.4	1.36	1.87	1.78
Average value:							1.35	1.85	1.78

**Table 6. Comparison of experimental results with values calculated according to various codes (slabs with shear reinforcement)**

Slab	$f_c$ [MPa]	$\Psi_{\text{exp, max}}$ [rad]	$V_{\text{exp}}$ [kN]	$V_{\text{EC2}}$ [kN]	$V_{\text{ACI}}$ [kN]	$V_{\text{MC}}$ [kN]	$V_{\text{exp}}/V_{\text{EC2}}$	$V_{\text{exp}}/V_{\text{ACI}}$	$V_{\text{exp}}/V_{\text{MC}}$
S2-1	43.1	0.02274	393.9	432.1	340.7	377.2	0.91	1.16	1.04
S2-2	45.2	0.02128	361.3	435.0	342.7	386.3	0.83	1.05	0.94
S2-3	42.7	0.02053	385.2	431.6	340.3	385.1	0.89	1.13	1.00
Average value:							0.88	1.11	0.99

specific weight of concrete, the value obtained is added to the one obtained by experiment, and thus the real punching force is obtained [13]. However, as the slabs of small thickness were used in this research, the influence of self-weight was neglected during definition of punching force results.

#### 4.2. Slabs without shear reinforcement

The comparison of punching forces obtained by experiments and through various calculation models is presented in Table 5 for slabs without shear reinforcement. The compressive strength values for concrete, as presented in this table, correspond to the values given in Table 4, i.e. these are the compressive strength values for concrete slabs that are estimated for the day of testing. It can be noticed that all design models under study are quite conservative in the estimation of punching force, i.e. they underestimate the real load carrying capacity of slabs. Thus, the most conservative model is the design model ACI 318, which is followed by MC 2010, while the results closest to the ones obtained by experiment are obtained by means of the EC 2 model. It should be noted that, if the specimen-size related ratio  $k$  from expression (5) is included in the calculation with the real value (rather than with the limit maximum value of 2.0), then the results obtained using EC 2 would be even more accurate, and the ratios of experimental to design values would become very close to 1. Safety ratios for materials are also used in the design process, and they additional shift design values to the side of safety.

#### 4.3. Slabs with shear reinforcement

The first of the three shear reinforcement perimeters was placed at 4.5 cm away from the column face, while the distance between individual perimeters was 7.0 cm, as shown in figure

8. Therefore, the total shear reinforcement area that is used in expressions (14), (16) and (17) is equal for all three design models, and amounts to 4.48 cm<sup>2</sup>.

The comparison of experimental and design punching forces for slabs with shear reinforcement is shown in Table 6. It can be seen that the slab punching forces are estimated relatively well using the design models MC 2010 and ACI 318. At that, the result of ACI 318 shifts for an average of 11 % to the side of safety, while MC 2010 slightly overestimates (for 1 %) the carrying capacity of slabs. Greater error on the side of safety in case of ACI 318 is due to the fact that in this model the shear strength of concrete in slabs with shear reinforcement has to be reduced by 50 % compared to this strength in the case of slabs without shear reinforcement. In the case of EC 2, this reduction amounts to 25 %, while in the case of MC 2010 it is included in design model via an increase in the inclination angle of the slab. The comparison of experimental results and the design model EC 2 reveals that this model overestimates the shear strength of slabs with shear reinforcement, with an average error of 12 %. Although this result is unfavourable, a satisfactory level of safety would be obtained even in this case through the use of safety ratios for materials in the standard design procedure.

### 5. Conclusion

A historic development of the structural system formed of slabs supported only on columns is described in the paper, together with the slab punching issue, which is a significant aspect in the design of such system. Three distinct slab punching design models are also presented: Eurocode 2, ACI Code 318, and fib Model Code 2010. In addition, the experimental research on slabs with and without shear reinforcement is described. A total of six relatively thin slabs (12.5 cm in thickness), three with and

three without shear reinforcement, were tested. The objective of the research was to expand the existing base of experimental research projects related to slab punching, as no tests of similarly thick slabs with shear reinforcement were found in the existing literature. A further objective was to estimate and compare the mentioned slab punching design models based on experimental research results.

All studied design models for slabs without shear reinforcement were revealed to be conservative, i.e. it was established that they underestimate the real carrying capacity of slabs subjected to punching shear. The most accurate prediction of punching forces was achieved using the expression according to EC 2. However, even better predictions can be achieved by this model by neglecting the prescribed ratio limitation that takes into account the specimen size ( $k \leq 2,0$ ). The most conservative results were obtained when the model ACI 318 was used, which is quite expected as this model involves one parameter only – the compressive strength of concrete, while it neglects parameters such as the reinforcement ratio and size effect. The model MC 2010 gives values that are somewhat less conservative than those provided by ACI 318. Here it should be noted that, out of the models under study, only the model MC 2010 is based on the observation of slab mechanics (kinematics). More precisely, the width of the critical shear crack is considered to be dependent on the inclination angle (rotation) of the slab [17]. Nevertheless, in the context of the relatively low thickness of slabs used in this research, we should bear in mind that the punching force results are highly sensitive to the specimen size effect. In other words, reduction in slab thickness results in relatively higher forces at which punching shear occurs and, as a consequence, the design models are more conservative.

Slabs strengthened with shear reinforcement exhibited punching shear forces that were on an average 17 % greater compared to the slabs without shear reinforcement. Furthermore, a 36 % increase can be observed in the deformation capacity of slabs, i.e. in the deflection and inclination angles. The design model ACI 318 has once again proven to be the most conservative

in the prediction of punching strength for slabs with shear reinforcement, while the model EC 2 overestimates the capacity of these slabs. The result obtained using the model ACI 318 is not surprising considering that, according to ACI 318, the contribution of concrete to the total resistance is reduced by 50 % in the case of slabs with shear reinforcement, when compared to this resistance in slabs without shear reinforcement. In the case of EC 2 model, this reduction amounts to 25 %, which finally led to an average error of 12 % in prediction of the specimen failure force (on the side of uncertainty). The design model MC 2010 does not provide for reduction in the contribution of concrete to the total shear resistance of slabs with shear reinforcement in the way this reduction is provided for in the models EC 2 and ACI 318. In this case, the contribution of concrete reduces with an increase in the critical shear crack width, i.e. with an increase in the inclination angle of the slab. In this research, the best correspondence with experimental results was obtained using the model MC 2010. Out of three specimens with shear reinforcement, this model overestimated the carrying capacity in one specimen only, which led to an average error of 1 % on the side of uncertainty. It should be noted that the efficiency of shear reinforcement anchoring is rather questionable in the tested slabs, because of their small thickness. A more accurate validation of experimental results would be made possible by the conduct of similar experiments on slabs of greater thickness strengthened with this type of shear reinforcement, and with other usual types of this reinforcement.

## Acknowledgements

The authors wish to acknowledge the financial support of the 7<sup>th</sup> Framework Programme of the European Community "Innovative Reuse of All Tyre Components in Concrete" under contract number 603722. The authors gratefully acknowledge all the participants in the above mentioned project with special thanks to colleagues from Faculty of Civil Engineering Zagreb - Department of Materials and company Gradmont d. o. o.

## REFERENCES

- [1] Wood, J.G.M.: *Pipers Row Car Park Wolverhampton: Quantitative Study of the Causes of the Partial Collapse on 20th March 1997*, 1997.
- [2] Sacramento, P.V.P., Ferreira, M.P., Oliveira, D.R.C., Melo, G.S.S.A.: Punching strength of reinforced concrete flat slabs without shear reinforcement, *Ibracon Structures and Materials Journal*, 5 (2012) 5, pp. 659–674.
- [3] Regan, P.E.: *Behaviour Of Reinforced Concrete Flat Slabs*, CIRIA Report No. 89, Construction Industry Research and Information Association, London, 1981.
- [4] Gasparini, D.A.: Contributions of C. A. P. Turner to Development of Reinforced Concrete Flat Slabs 1905. - 1909., *Journal of Structural Engineering*, 128 (2002) 10, pp. 1243–1252, doi:10.1061/(ASCE)0733-9445(2002)128:10(1243),
- [5] Furst, A., Marti, D.: Robert Maillart's Design Approach for Flat Slabs, *Journal of Structural Engineering*, 123 (1997) 8, pp. 1102–1110.
- [6] Kierdorf, A.: Early Mushroom Slab Construction in Switzerland, Russia and the U.S.A. – A Study in Parallel Technological Development, Proceedings of the Second International Congress on Construction History, 2006: pp. 1793–1807.

- [7] Kunz, J., Fernández Ruiz, M., Muttoni, A.: Enhanced safety with post-installed punching shear reinforcement, Walraven, J.C., Stoeckhorst, D. (Eds.), *Tailor Made Concrete Structures - New Solutions for Our Society*, Taylor and Francis Group, 2008: pp. 679–684.
- [8] Birkle, G., Dilger, W.H.: Shear Strength of Slabs with Double-Headed Shear Studs in Radial and Orthogonal Layouts, *ACI Special Publication 265-23*, American Concrete Institute, 2009: pp. 499–510.
- [9] Birkle, G., Dilger, W.H.: Influence of slab thickness on punching shear strength, *ACI Structural Journal*, 105 (2008) 2, pp. 180–188.
- [10] Stein, T., Ghali, A., Dilger, W.: Distinction between Punching and Flexural Failure Modes of Flat Plates, *ACI Structural Journal*, 104 (2007) 3, pp. 357–365.
- [11] Dilger, W., Birkle, G., Mitchell, D.: Effect of Flexural Reinforcement on Punching Shear Resistance, *ACI Special Publication 232-4*, American Concrete Institute, 2005: pp. 57–74.
- [12] Hegger, J., Ricker, M., Sherif, A.G.: Punching strength of reinforced concrete footings, *ACI Structural Journal*, 106 (2009) 5, pp. 706–716.
- [13] Beutel, R., Hegger, J.: The effect of anchorage on the effectiveness of the shear reinforcement in the punching zone, *Cement and Concrete Composites*, 24 (2002) 6, pp. 539–549, doi:10.1016/S0958-9465(01)00070-1.
- [14] Fernández Ruiz, M., Muttoni, A.: Applications of critical shear crack theory to punching of reinforced concrete slabs with transverse reinforcement, *ACI Structural Journal*, 106 (2009) 4, pp. 485–494.
- [15] Lips, S., Fernández Ruiz, M., Muttoni, A.: Experimental Investigation on Punching Strength and Deformation Capacity of Shear-Reinforced Slabs, *ACI Structural Journal*, 109 (2012) pp. 889–900.
- [16] Muttoni, A., Schwartz, J.: Behaviour of beams and punching in slabs without shear reinforcement, *IABSE Colloquium*, Zurich, 1991: pp. 703–708.
- [17] Muttoni, A.: Punching shear strength of reinforced concrete slabs without transverse reinforcement, *ACI Structural Journal*, 105 (2008) 4, pp. 440–450.
- [18] European Committee for Standardization: Eurokod 2: Design of concrete structures - Part 1-1: General rules and rules for buildings, (2004) pp. 225.
- [19] ACI Committee 318: Building code requirements for structural concrete and commentary (ACI 318-14), (2014) pp. 525.
- [20] Federation internationale du beton: Model Code for Concrete Structures 2010, (2013) pp. 410.
- [21] HZN: HRN EN ISO 15630-1:2010. Čelik za armiranje i prednapinjanje betona - Metode ispitivanja - 1. dio: Armaturne šipke, valjana žica i žica, (2010).
- [22] HZN: HRN EN 12390-3:2012. Ispitivanje očvrsluoga betona - 3. dio: Tlačna čvrstoća ispitnih uzoraka., (2012).
- [23] HZN: HRN EN 12390-13:2013. Ispitivanje očvrsluoga betona - 13. dio: Određivanje sekantnog modula elastičnosti pri tlaku, (2013).
- [24] HZN: HRN EN 12390-6:2010. Ispitivanje očvrsluoga betona - 6. dio: Vlačna čvrstoća cijepanjem, (2010).